Interactions of Phenol and Indole with Metal Ions in the Gas Phase: Models For Tyr and Trp Side-Chain Binding

Victor Ryzhov and Robert C. Dunbar*

Contribution from the Department of Chemistry, Case Western Reserve University, Cleveland, Ohio 44106

Received September 14, 1998

Abstract: The binding energies of a number of metal cations with phenol and indole in the gas phase were studied experimentally by radiative association kinetics analysis, supplemented by density functional calculations. Radiative association kinetics measurements were carried out in the Fourier transform ion cyclotron resonance mass spectrometer. Reaction in most cases resulted in adduct formation often followed by sequential addition of a second neutral molecule to the ion. The association kinetics were analyzed to yield binding energy values either by using a variational transition state theory-based approach, incorporating quantum-chemical calculations of vibrational frequencies and infrared intensities, or by using the semiquantitative standard hydrocarbon approach. The competitive collision-induced dissociation (CID) technique was used to confirm the order of relative binding energies for several complexes. Calculations of the structures and energies of a number of complexes were performed, by means of the B3LYP-density functional approach, both to complement and compare with the experimental binding energies and also to address the question of π versus heteroatom bonding. With phenol, the two binding sites are close in energy for nontransition metals, but the π-site is relatively more favorable for Fe^+ and probably Cr^+. Experimental, literature, and calculated values were combined to give best-estimate binding energies for a variety of metal ions. For the nontransition-metal ions characterized, phenol binding is similar to benzene binding, whereas for Cr^+ and especially Fe^+ phenol binding is stronger than benzene binding. With indole, binding is always enhanced by ∼5−10 kcal mol^{-1} relative to benzene. Formation of dimer ML_2^+ complexes followed patterns similar to those of previous benzene results, except that phenol dimer complexes with Mg^+ and Al^+ were unexpectedly observed, suggesting involvement of an oxygen binding site in these cases.

Introduction

The interaction of metal ions with organic π-systems has been a central theme of gas-phase ion chemistry studies for more than two decades. (For a few examples among many, see refs 1,2.) This field has recently become interesting from a new perspective, as it relates to the understanding of cation−π interactions in both structural and mechanistic aspects of biological systems. Propelled substantially by work of the Dougherty group,[3,4] there is rapidly expanding appreciation of ways that cation−π interactions involving proteins and other components of biological systems may be important, for instance, in governing protein structural organization[3−9] or the functioning of ionic channels in membranes.[10,11] Thinking about these questions draws heavily on both experimental and theoretical studies of fundamental ion−neutral interactions between defined cations and the molecular building blocks of larger biological molecules and assemblies. Characterizing these interactions in the gas phase is an important part of building a basis of information about the nature and strength of these interactions. The research described here contributes to this by a combination of gas-phase experimental study and quantum-chemical computations of the fundamental interactions of various cations with the aromatic groups constituting the side chains of tyrosine (Tyr) and tryptophan (Trp). These aromatic amino acid side-chain structures are shown as **1** and **2**; when R = H, these are phenol and indole, respectively.

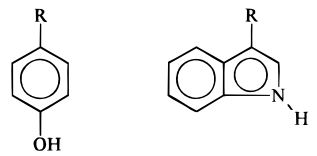

1 **2**

A great deal of attention has been paid to metal cation−π interacting systems involving the alkali cations of greatest biological interest, notably Na^+ and K^+, as well as some closed-shell nonmetallic cations like alkylammonium ions; these areas have been comprehensively reviewed[3,4] and continue to be investigated actively. Recent examples include both quantum-chemical and experimental studies. The nature and strength of binding and the roles of electrostatic and polarization terms in

* To whom correspondence should be addressed.

(1) Russell, D. H. *Gas-Phase Inorganic Chemistry*; Plenum Press: New York, 1989.
(2) Freiser, B. S. *Organometallic Ion Chemistry*; Kluwer Academic Publishers: Dordrecht, 1996.
(3) Ma, J. C.; Dougherty, D. A. *Chem. Rev.* **1997**, *97*, 1303.
(4) Dougherty, D. A. *Science* **1996**, *271*, 163.
(5) DeVos, A. M.; Ultsch, M.; Kossiakoff, A. A. *Science* **1992**, *255*, 306−312.
(6) Karlin, A. *Curr. Opin. Neurobiol.* **1993**, *3*, 299−309.
(7) Raves, M. L.; Harel, M.; Pang, Y. P.; Silman, I.; Kozikowski, A. P.; Sussman, J. L. *Nat. Struct. Biol.* **1997**, *4*, 57−63.
(8) Stauffer, D. A.; Karlin, A. *Biochemistry* **1994**, *33*, 6840−9.
(9) Mitchell, J. B.; Nandi, C. L.; McDonald, I. K.; Thornton, J. M.; Price, S. L. *J. Mol. Biol.* **1994**, *239*, 315−331.
(10) Zhong, W.; Gallivan, J. P.; Zhang, Y.; Li, L.; Lester, H. A.; Dougherty, D. A. *Proc. Natl. Acad. Sci. U.S.A.* **1998**, *95*, 12088.
(11) Donini, O.; Weaver, D. F. *J. Comput. Chem.* **1998**, *19*, 1515.

10.1021/ja983272z CCC: $18.00
Published on Web 03/02/1999

the potential, have been explored theoretically.[11−22] Experimental evidence is accumulating for such cation−π interactions in complex systems, for which refs 3, 16, 23, 24 provide examples.

Less attention has thus far been directed to systems involving other metal ions, but these are also of interest and have been studied in various ways. For instance, crystal structures of bis(tyrosinato) copper(II),[25] bis(tyrosinato) Pd(II)[26] and (Gly Leu-Tyr) Cu(II),[27] have shown the metal ion to be located within bonding distance of the aromatic ring. In solution, planar complexes of Ni^{2+} and Pd^{2+} with amino acids and di- and tripeptides exhibit a dramatic increase in the population of the conformation that has a side-chain situated over a coordinated metal ion (Structure 1), if the chelating molecule contains an

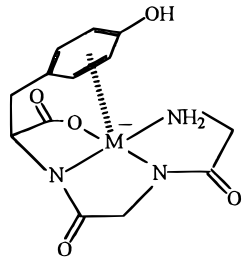

1

aromatic side chain.[28] In the gas phase, CID of complexes of singly deprotonated oligopeptides with doubly charged metal ions leads to predominant loss of fragments that do not contain aromatic side chains, suggesting strong participation of the aromatic groups in metal ion binding.[29] Lei and Amster[30] studied reactions of Cu^+ ions with the 20 common amino acids and found that for Tyr and Trp the only products are the association adducts, whereas for other amino acids fast ion−molecule reactions more complicated than association reactions typically dominate. A possible explanation for this observation is that the particularly strong bonding between the metal ion and the aromatic fragments makes the association channel especially favorable relative to other reactive channels.

An interesting feature of Tyr and Trp side chains is the presence of multiple side-chain binding sites (the π-site along with the oxygen lone-pair site on the phenol side chain of Tyr, two π-sites along with the nitrogen lone-pair site on the indole side chain of Trp). It is not obvious what the preferred binding sites will be for different metal ions. Hu et al.,[29] in a study of ion fragmentation for a number of chelated divalent metal ions, did not rule out the possibility of chelating the metal ion in oligopeptide complexes by either binding site of Tyr (Structures 2 and 3).

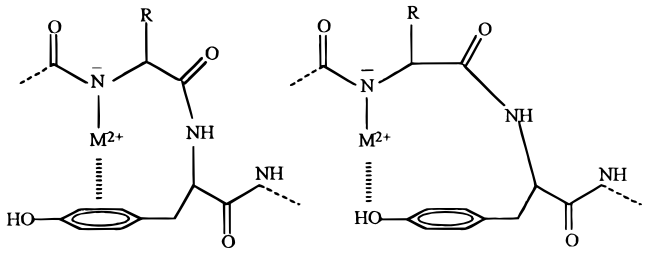

2 **3**

Experiments giving binding energy information do not directly address questions of alternative binding sites. Calculations offer an increasingly powerful way to compare possible binding sites. In the case of indole, the Dougherty group's recent ab initio results for sodium ions,[4,13] extended by our group to Al^+ and Mg^+,[21] have shown quite conclusively that the nitrogen binding site in indole does not compete successfully with π-face binding and that the phenyl site is favored over the pyrrole site. For phenol, the Dougherty group's Na^+ results[13] suggested the oxygen site to be favored by 0.5 kcal mol^{-1} over the ring site. Here we explore this choice of sites computationally for a variety of metal ions. We also consider the possible indirect interpretation of our experimental observations for assigning the site of metal ion attachment to phenol.

There are still many aspects of metal ion/aromatic side chain interactions open to clarification by gas-phase experiments and by the increasingly powerful resources of quantum-chemical calculations. The present study focuses principally on the experimental study of the relative binding energies of a varied set of metal ions with phenol and indole, using the radiative association kinetics approach in the Fourier transform ion-trapping mass spectrometer. Accompanying quantum-chemical calculations are used in three different contexts: (1) to provide molecular properties needed in the radiative association data analysis, (2) to complement the experimental binding energy results, and (3) to address the experimentally difficult question of the relative stabilities of different binding sites.

Interactions of different metal ions with various aromatic ligands have been a subject of recent interest in our labora tory.[21,31−39] Several experimental approaches have been explored, based on association and dissociation kinetics involving metal ion complexes trapped in the FT-ICR cell,[37] with recent

(12) Mecozzi, S.; West, A. P., Jr.; Dougherty, D. A. *J. Am. Chem. Soc.* **1996**, *118*, 2307.
(13) Mecozzi, S.; West, A. P., Jr,; Dougherty, D. A. *Proc. Natl. Acad. Sci. U.S.A.* **1996**, *93*, 10566.
(14) Miklis, P. C.; Ditchfield, R.; Spencer, T. A. *J. Am. Chem. Soc.* **1998**, *120*, 10482.
(15) Cubero, E.; Luque, F. J.; Orozco, M. *Proc. Natl. Acad. Sci. U.S.A.* **1998**, *95*, 5976.
(16) Kim, K. S.; Lee, J. Y.; Lee, S. J.; Ha, T.-K.; Kim, D. H. *J. Am. Chem. Soc.* **1994**, *116*, 7399.
(17) Lee, J. Y.; Lee, S. J.; Choi, H. S.; Cho, S. J.; Kim, K. S.; Ha, T.-K. *Chem. Phys. Lett.* **1995**, *232*, 67.
(18) Caldwell, J. W.; Kollman, P. A. *J. Am. Chem. Soc.* **1995**, *117*, 4177.
(19) Pullman, A.; Berthier, G.; Savinelli, R. *J. Comput. Chem.* **1997**, *18*, 2012.
(20) Pullman, A.; Berthier, G.; Savinelli, R. *J. Am. Chem. Soc.* **1998**, *120*, 8553.
(21) Dunbar, R. C. *J. Phys. Chem. A* **1998**, *102*, 8946.
(22) Stöckigt, D. *J. Phys. Chem. A* **1997**, *101*, 3800.
(23) Choi, H. S.; Suh, S. B.; Cho, S. J.; Kim, K. S. *Proc. Natl. Acad. Sci. U.S.A.* **1998**, *95*, 12094.
(24) Murayama, K.; Aoki, K. *Inorg. Chim. Acta* **1998**, *281*, 36.
(25) VanDerHelm, D.; Tatsch, C. E. *Acta Crystallogr., Sect. B* **1972**, *28*, 2307.
(26) Sarat, M.; Jesowski, M.; Kozlowski, H. *Inorg. Chim. Acta* **1979**, *37*, L511.
(27) Franks, W. A.; VanDerHelm, D. *Acta Crystallogr. Sect. B* **1971**, *27*, 1299.
(28) Vestues, P. I.; Martin, R. B. *J. Am. Chem. Soc.* **1980**, *102*, 7906.
(29) Hu, P.; Sorensen, C.; Gross, M. L. *J. Am. Soc. Mass Spectrom.* **1995**, *6*, 1079.
(30) Lei, Q. P.; Amster, I. J. *J. Am. Soc. Mass Spectrom.* **1996**, *7*, 722.
(31) Dunbar, R. C.; Uechi, G. T.; Solooki, D.; Tessier, C. A.; Youngs, W.; Asamoto, B. *J. Am. Chem. Soc.* **1993**, *115*, 12477.
(32) Lin, C.-Y.; Dunbar, R. C. *Organometallics* **1997**, *16*, 2691.
(33) Lin, C.-Y.; Dunbar, R. C. *J. Phys. Chem.* **1995**, *99*, 1754.
(34) Ho, Y.-P.; Yang, Y.-C.; Klippenstein, S. J.; Dunbar, R. C. *J. Phys. Chem.* **1997**, *101*, 3338.
(35) Faulk, J. D.; Dunbar, R. C. *J. Am. Chem. Soc.* **1992**, *114*, 8596.
(36) Dunbar, R. C.; Klippenstein, S. J.; Hrušák, J.; Stöckigt, D.; Schwarz, H. *J. Am. Chem. Soc.* **1996**, *118*, 5277.
(37) Dunbar, R. C. New Approaches to Ion Thermochemistry via Dissociation and Association. In *Advances in Gas-Phase Ion Chemistry*; Babcock, L. M., Adams, N. G., Eds.; JAI Press: Greenwich, CT, 1996; Vol. 2; p 87.

attention focusing on the kinetics of radiative association.[40] Formation of an ion−ligand adduct by means of radiative association with subsequent analysis of the kinetics (the RA kinetics approach) has proven to be a useful tool for quantitative estimations of binding energies of complexes.[32,34,36,37,41,42] Taking advantage of the power of variational transition state theory (VTST)[36,41] RA kinetics analysis has given binding energy values of precision comparable to alternative techniques. This approach is applied here, complemented by quantum-chemical theoretical calculations, to characterize the interaction energy of a variety of singly charged metal cations with phenol and indole.

An intrinsic limit of the RA kinetics approach is that the experimental regime is limited to systems with association efficiencies from 0.001 to ~0.5. Reactions slower than this are hard to observe, while those faster than this come close to the collisional saturation limit. Varying the temperature can extend the range of accessible systems,[43] although temperatures different from room temperature were not used in the present study.

The computational effort is substantial for fully detailed analysis of RA kinetics data, although the availability, power, and convenience of the relevant computer programs is improving steadily. A simple generic approach to approximate data analysis, known as the "standard hydrocarbon" model,[44−46] is useful for semiquantative interpretations of RA observations.[47] This is applied below to the present results for comparison with the fully detailed analysis and is also used to analyze several cases where the detailed analysis was not carried out.

Other experimental approaches to determining ion−neutral binding energies are in active use, including threshold photodissociation,[48−50] photodissociation kinetics analysis,[33,35,37] thermal infrared blackbody dissociation,[37,51,52] ligand exchange equilibrium,[53] threshold collision-induced dissociation (CID),[54−56] and competitive collisional dissociation of mixed $ML_1L_2^+$ complexes (the "kinetic method").[57,58]

Experimental Section

Experiments were performed on an FT-ICR spectrometer with a 2.54-cm cubical cell. The details of the instrument are described elsewhere.[46,52] Neutrals were introduced into the cell through leak valves (Varian). The pressure of the neutrals varied from 5×10^{-9} to 5×10^{-7} Torr. The ion gauge pressure readings were calibrated by ion−molecule reactions (see below). Metal ions were formed by laser desoption−ionization by focusing a pulsed YAG laser (Lumonics) beam on the metal target located behind the cell near the hole in the trapping plate. Cr^+ and Fe^+ were produced from stainless steel, Na^+ from NaCl, K^+ from a paint residue on the probe tip, and other ions from the pure metals. After ion formation a thermalization period allowing at least 20 ion−neutral collisions was provided by a pulse of nitrogen gas introduced through a pulsed valve (General Valve). After that the unwanted ionic species were removed by a series of ejection pulses and allowed to react for a time which ranged from 200 ms to 90 s, following which the extent of association was measured as a function of the reaction time.

The ion gauge pressure readings were calibrated by ion−molecule reactions. We have not found feasible reactions of phenol or indole with well-known rates. It was possible, however, to find several very fast association, proton-transfer or charge-transfer reactions for each neutral. Assuming that the fastest observable reaction proceeds with collisional rate, which is usually not a bad assumption,[59] pressure calibration was possible. For phenol, association with Fe^+ turned out to be the fastest reaction. For indole, the exothermic charge transfer from NO^+ gave the fastest rate. The deviations from the pressure values derived from these ion−molecule reactions, versus those obtained directly from the ion gauge readings divided by the gauge factors, were quite substantial, approximately a factor of 1.6 for phenol and of 2.1 for indole. Subsequently, our confidence in these numbers was increased by observing several fast association reactions with efficiencies in the range of 0.9 to 1, using these pressure calibrations.

Modeling Details

Modeling of the radiative association kinetics is central to the interpretation of experimental results as a route to binding energy information. An association reaction can be analyzed in terms of the detailed mechanism

$$A^+ + B \underset{k_b}{\overset{k_f}{\rightleftharpoons}} (AB)^{+*} \xrightarrow{k_r} AB^+ \qquad (1)$$

$$(AB)^{+*} \xrightarrow{[M],\ k_c\beta} AB^+$$

where k_f is the bimolecular rate constant for collisional complex formation,[60] k_b is the unimolecular redissociation rate constant, k_r is the unimolecular rate constant for IR photon emission from the energized complex, and $k_c\beta$ is the bimolecular rate constant for collisional stabilization of AB^{+*} by collision with neutral M. AB^{+*} is the metastable collision complex.

Modeling based on variational transition-state theory (VTST) along with quantum chemical calculations of IR frequencies and intensities has given excellent results in terms of calculating and combining the microscopic rate constants to predict accurate kinetics.[41,61] The kinetics are treated by a VTST approach incorporating convolutions over a thermal distribution of energies and angular momenta for the reactants and over the distribution of angular momenta and energies of the complex. This approach has been described in detail.[41,61]

Individual IR absorption intensities and vibrational frequencies were calculated for several of the complexes as described in Computational Methods. Values of frequencies and intensities from some of these calculations not previously published are given in Tables 2, 3, and 5−7.

(38) Dunbar, R. C.; Uechi, G. T.; Asamoto, B. *J. Am. Chem. Soc.* **1994**, *116*, 2466.
(39) Pozniak, B. P.; Dunbar, R. C. *J. Am. Chem. Soc.* **1997**, *119*, 10439−10445.
(40) Dunbar, R. C. Review: Ion-Molecule Radiative Association. In *Current Topics Ion Chemistry and Physics*; Ng, C. Y., Baer, T., Powis, I., Eds.; Wiley: New York, 1994; Vol. II.
(41) (a) Klippenstein, S. J.; Yang, Y.-C.; Ryzhov, V.; Dunbar, R. C. *J. Chem. Phys.* **1996**, *104*, 4502. (b) Ryzhov, V. Ph.D. Dissertation, Case Western Reserve University, Cleveland, OH, 1998.
(42) Cheng, Y. W.; Dunbar, R. C. *J. Phys. Chem.* **1995**, *99*, 10802.
(43) Ryzhov, V.; Yang, Y.-C.; Klippenstein, S. J.; Dunbar, R. C. *J. Phys. Chem. A* **1998**, *102*, 8865.
(44) Herbst, E.; Dunbar, R. C. *Mon. Not. R. Astron. Soc.* **1991**, *253*, 341.
(45) Dunbar, R. C. *Int. J. Mass Spectrom. Ion Processes* **1997**, *160*, 1.
(46) Dunbar, R. C. *Int. J. Mass Spectrom. Ion Processes* **1990**, *100*, 423.
(47) Ryzhov, V.; Dunbar, R. C. *Int. J. Mass Spectrom. Ion Processes* **1997**, *167/168*, 627−635.
(48) Afzaal, S.; Freiser, B. S. *Chem. Phys. Lett.* **1994**, *218*, 254.
(49) Sallans, L.; Laude, D. R.; Freiser, B. S. *J. Am. Chem. Soc.* **1989**, *111*, 865.
(50) Willey, K. F.; Cheng, P. Y.; Bishop, M. B.; Duncan, M. A. *J. Am. Chem. Soc.* **1991**, *113*, 4721.
(51) Lin, C.-Y.; Dunbar, R. C.; Haynes, C. L.; Armentrout, P. B.; Tonner, D. S.; McMahon, T. B. *J. Phys. Chem.* **1996**, *100*, 19659.
(52) Lin, C.-Y.; Dunbar, R. C. *J. Phys. Chem.* **1996**, *100*, 655.
(53) Uppal, J. S.; Staley, R. H. *J. Am. Chem. Soc.* **1982**, *104*, 1235.
(54) Schultz, R. H.; Armentrout, P. B. *J. Phys. Chem.* **1993**, *97*, 596.
(55) Chen, Y. M.; Armentrout, P. B. *Chem. Phys. Lett.* **1993**, *210*, 123.
(56) Meyer, F.; Khan, F. A.; Armentrout, P. B. *J. Am. Chem. Soc.* **1995**, *117*, 9740.
(57) Wesdemiotis, C.; Cerda, B. A. Presented at the 46th ASMS Conference on Mass Spectrometry and Allied Topics, Orlando, May 31−June 4, 1998.
(58) Cooks, R. G.; Patrick, J. S.; Kotiaho, T.; McLuckey, S. A. *Mass Spectrom. Rev.* **1994**, *13*, 287.
(59) Barker, R. A.; Ridge, D. P. *J. Chem. Phys.* **1976**, *64*, 4411.
(60) It is assumed here that every orbiting collision results in the formation of a metastable collision complex, although this is not necessarily true. See: Weddle, G.; Dunbar, R. C. *Int. J. Mass Spectrom. Ion Processes* **1994**, *134*, 73 for discussion of this possibility.
(61) Ryzhov, V.; Klippenstein, S. J.; Dunbar, R. C. *J. Am. Chem. Soc.* **1996**, *118*, 5462.

Table 1. Example Comparisons of Photon Emission Rates and Binding Energies from Standard Hydrocarbon Semiquantitative Estimation, and VTST/ab Initio Modeling, Both Applied to the Experimentally Observed Radiative Association Rate

system	k_r(StH) (s^{-1})	k_r(VTST) (s^{-1})	BE(StH)[a] (kcal mol^{-1})	BE(VTST)[a] (kcal mol^{-1})
Cr^+/benzene	32	16[b]	42.6	39.6[c]
Cr^+/phenol (ring)	38	49	49.2	46.2
Al^+/phenol (ring)	30	45	42.3	40.7
Na^+/indole	19	24	33.6	34.7

[a] VTST-derived binding energies are uncertain to perhaps ±10%, whereas standard hydrocarbon values certainly have larger, but hard-to-define uncertainties. [b] Calculated using vibrational frequencies and infrared intensities from ref 32. [c] From ref 32.

Several other complexes were analyzed by the VTST-based approach, using estimated parameters as follows: Mg^+/phenol was taken to have the same frequencies and intensities as calculated for Al^+/phenol; frequencies and intensities for Ca^+/indole and K^+/indole were the same as those calculated for Na^+/indole, except that the three low-frequency modes were scaled by $(BE/\mu)^{1/2}$ where BE is the binding energy and μ is the reduced mass of the metal ion/indole pair.

Unfortunately, ab initio calculations are inconvenient for routine work and become harder and less reliable for calculating IR radiative properties of larger systems (that is, more than 15 heavy atoms). At the same time, the potential surface for VTST calculations becomes increasingly complicated and difficult as the number of degrees of freedom increases. The standard hydrocarbon (StH) approach[44−46] avoids all such difficulties of detailed calculation by taking a generic view of hydrocarbon properties and assuming that the specific details of individual molecules will have only secondary importance in determining the radiative association kinetics of hydrocarbon-based reaction systems. Both the IR radiative properties (k_r) and the unimolecular reaction kinetics (k_b) are assumed to a first approximation to depend only on the number of degrees of freedom N of the A^+B^* complex, the reaction temperature, and the complex binding energy E_b.[45]

Table 1 shows a few comparisons of StH results and comparable results from the best available detailed modeling procedures. The comparison of IR photon emission rates gives the rates calculated from quantum-chemical IR frequencies and intensities, compared with the corresponding generic values used in StH modeling. It is evident that the generic assignments are useful within perhaps a factor of 2. The binding energy comparison compares the detailed modeling applied to experimental results on several systems, with the corresponding binding energies assigned from the StH scheme of ref 45. This suggests that StH binding energy values have semiquantitative usefulness as approximations to the full VTST/quantum-chemistry analysis within an uncertainty of ∼10%.

Computational Methods

Indole. All of the quantum-chemical calculations of frequencies, intensities, and binding energies used the GAUSSIAN 94 program package.[62] For the metal ion − indole systems with Na^+, Mg^+, and Al^+, ref 21 describes extensive maps of the binding energy surfaces calculated at the Hartree−Fock (HF) level with the 6-31G(d) basis set, corrected at the MP2 level for correlation, and corrected for the minor extent of geometry relaxation. Those calculations were considered reliable for comparison of different binding sites and comparison of different metals but were not designed for producing believable absolute binding energies. Comparable calculations for naphthalene were also reported. Other calculations of Na^+ binding to indole, as well as naphthalene, were previously reported at roughly comparable levels of theory.[4,13]

Table 2. Reactant-Molecule Vibrational Frequencies for Phenol and Indole. B3LYP-DFT Calculations for Phenol, HF Calculations for Indole

molecule	frequency[a]
phenol	257, 320, 440, 462, 568, 574, 679, 768, 848, 892, 929, 997, 1086, 1089, 1112, 1125, 1181, 1202, 1289, 1299, 1377, 1405, 1498, 1642, 1676, 1801, 1813, 3341, 3361, 3371, 3387, 3396, 4118
indole	242, 279, 440, 486, 603, 604, 654, 682, 683, 838, 842, 872, 903, 972, 1000, 1005, 1062, 1110, 1120, 1159, 1180, 1217, 1253, 1288, 1336, 1400, 1410, 1429, 1521, 1582, 1631, 1672, 1712, 1782, 1821, 3349, 3358, 3371, 3386, 3436, 3465, 3945

[a] Frequencies in cm^{-1}. Frequencies given here are unscaled but were scaled downward by 0.89 when used in the kinetics calculations described in the text.

Density functional calculations using the B3LYP hybrid functional to account for correlation and exchange may provide useful binding energies for large systems where basis set size is constrained, particularly in systems containing transition metals, and make it possible to use somewhat larger, more flexible basis sets than MP2 calculations. Accordingly, a further set of calculations using density functional (DFT) methods was performed here to get better binding energy comparisons with the present data. (However, as discussed below, the work of Stöckigt on Al^+,[22] corroborated by our present results for several metal ions, suggests a systematic ∼5 kcal mol^{-1} underestimate of the absolute binding energies calculated by this method, so that we will be very circumspect in using these calculated values in any absolute binding energy context.) In these DFT calculations the basis set was 6-31+G-(d) on carbon and nitrogen, 6-31g(d) on hydrogen, and 6-311+g(d) on the metal. The potassium basis was the 6-31G(d) basis of Rassolov et al.,[63] which was augmented by splitting the polarization d shell into two d shells, and by adding a diffuse sp^3 shell. The geometry of each complex was fully optimized at the most stable (phenyl-ring-bound) structure. Basis set superposition errors (BSSE) estimated using the geometry-relaxed scheme of Xantheas[64] were small. For example, the BSSE correction weakened the binding by 0.2, 0.4, and 0.6 kcal mol^{-1} for K^+, Al^+, and Cr^+, respectively. To get an estimate of typical vibrational zero-point energy (ZPE) corrections, vibrational frequencies at the HF level were calculated for neutral indole (Table 2) and for the Na^+ complex (Table 3). The ZPE correction for this case acts to weaken the binding by 0.8 kcal mol^{-1}. For the other indole complexes, ZPE effects were assumed here to weaken the binding by 1.0 kcal mol^{-1}. Some indication of the basis set adequacy was obtained by comparison with calculations without diffuse functions on the carbons and using the 6-31+g(d) basis on the metal. With this smaller basis, the BSSE was much larger (more than 2 kcal mol^{-1} for the alkalis and more than 5 kcal mol^{-1} for the other metals), but the final binding energy values obtained after making a BSSE correction were the same as with the larger basis within about 1 kcal mol^{-1}.

Phenol. Similar B3LYP-DFT methods were used for the metal ion/phenol calculations. The normal phenol basis set was 6-31+G(d) on the heavy atoms, 6-31G(d) on hydrogen, augmented with polarization functions on the hydroxylic hydrogen. The normal metal atom basis was 6-311+G(d). The potassium basis was as described above for indole. Exceptions to this basis were as follows: (a) for the iron calculations, and for all of the vibrational frequency/intensity calculations, no diffuse functions were used on the carbons so that the carbon atom basis was 6-31G(d); (b) the vibrational frequencies and intensities used in the kinetics analysis of Mg^+ and Al^+ data were calculated using a smaller 6-31G(d) basis on the metal atoms.

For Mg^+ and Al^+ calculations expansion of the metal atom basis set from 6-31G(d) to 6-311+G(d) actually made little difference to

(62) Frisch, M. J.; Trucks, G. W.; Schlegel, H. B.; Gill, P. M. W.; Johnson, B. G.; Robb, M. A.; Cheeseman, J. R.; Keith, T.; Petersson, G. A.; Montgomery, J. A.; Raghavachari, K.; Al-Laham, M. A.; Zakrzewski, V. G.; Ortiz, J. V.; Foresman, J. B.; Cioslowski, J.; Stefanov, B. B.; Nanayakkara, A.; Challacombe, M.; Peng, C. Y.; Ayala, P. Y.; Chen, W.; Wong, M. W.; Andres, J. L.; Replogle, E. S.; Gomperts, R.; Martin, R. L.; Fox, D. J.; Binkley, J. S.; Defrees, D. J.; Baker, J.; Stewart, J. P.; Head-Gordon, M.; Gonzalez, C.; Pople, J. A., GAUSSIAN 94, Gaussian, Inc.: Pittsburgh, PA, 1995.

(63) Rassolov, V.; Pople, J. A.; Ratner, M.; Windus, T. L. *J. Chem. Phys.* **1998**, in press.

(64) Xantheas, S. S. *J. Chem. Phys.* **1996**, *104*, 8821.

Table 3. Complex-Ion Vibrational Frequencies, Intensities, and Rotational Constants for $IndNa^+$, HF/6-31G* Calculations (π-Binding Site on the Phenyl Ring Side)

frequency[a] (intensity)		
3239(10), 78(7.5), 101(3.2), 200(39), 254(14), 280(0.30), 441(4.4), 486(13), 599(0.54), 648(5.7), 677(13), 680(15), 703(135), 831(2.0), 835(22), 896(27), 913(203), 973(0.14), 998(6.6), 1023(3.0), 1091(1.9), 1104(6.2), 1125(8.9), 1154(3.2), 1182(28), 1221(17), 1248(2.6), 1289(2.3), 1334(7.3), 1400(41), 1407(11), 1430(4.2), 1521(8.4), 1585(48), 1623(68), 1656(1.6), 1695(26), 1755(7.4), 1793(4.9), 3373(0.14), 3379(0.06), 3390(2.4), 3401(1.2), 3453(2.4), 3479(0.09), 3914(136)		
rotational constants		
0.072	0.038	0.036

[a] Frequencies and rotational constants in cm^{-1}, intensities in km/mole. Frequencies given here are unscaled but were scaled downward by 0.89 when used in the kinetics calculations described in the text.

Table 4. Radiative Association of Metal Ions with Phenol and Indole. Kinetic Data for Addition of the First and Second Ligands and Binding Energies Derived for the First Ligand

neutral	ion	k_f[a]	k_{ra}[b]	$\Phi(ML^+)$[c]	BE[e]	ML_2^+[d]
phenol	Mg^+	24.3	1.5	0.063	38.2[k]	slow[g]
	Al^+	23.1	1.2	0.05[i]	37.5[i,k]	slow[g]
	Cr^+	18.6	4.3	0.23	49.3	fast[f]
	Fe^+	18.1	18	~1	>57	fast[f]
indole	Na^+	31.1	0.27	0.010	32.9	no[h]
	Mg^+	31.0	14.0	0.5	48[m]	no[h]
	Al^+	29.0	14.0	0.5	48[m]	no[h]
	K^+	25.2	0.006	0.0003	25.0	no[h]
	Ca^+	24.8	1.2	0.05	36	fast[f]
	Cr^+	22.7	22.0	~1	>48[m]	fast[f]
	Fe^+	22.1	21.0	~1	>48[m]	fast[f]
	Mo^+	18.6	6.0	0.3	>48[m]	fast[f]

[a] Calculated dipole-corrected Langevin orbiting collision rate, 10^{-10} cm^3 $molecule^{-1}$ s^{-1}. [b] Measured association rate constant, 10^{-10} cm^3 $molecule^{-1}$ s^{-1}. [c] Fraction of collisions giving stabilized association product ML^+, calculated as k_f/k_{ra}. [d] Rate constant for formation of ML_2^+ from ML^+, cm^3 $molecule^{-1}$ s^{-1}. [e] "Experimental" binding energy calculated from k_{ra}, kcal mol^{-1} using the full VTST calculation except where otherwise indicated. VTST-derived binding energies are uncertain to perhaps ±10%, whereas StH values certainly have larger, but hard-to-define uncertainties. [f] Efficiency 50−100%. [g] Efficiency greater than 1% but less than 10%. [h] Efficiency less than 2%. [i] Al^+ forms AlO^+ in amounts comparable with association. The binding energy estimate given is calculated without considering this competing channel and is thus probably too low by an amount of the order of 2 kcal mol^{-1}. [k] Analyzed by assuming attachment at the oxygen site. [m] Semiquantitative binding energy estimate based on StH.

binding energies or geometries. On the other hand, the inclusion of diffuse orbitals on the carbons gave significant changes. Comparison with results omitting these orbitals showed that the addition of diffuse orbitals to the carbon atom basis gave negligible changes in geometry but reduced the binding energies to the ring site by between 1 and 2.5 kcal mol^{-1} (after correcting for BSSE); moreover, the addition of these carbon diffuse orbitals greatly reduced the calculated BSSE in all cases (by a factor of 3 or 4), suggesting that these diffuse orbitals in the π-system constitute an important component of the basis.

The geometries were optimized for both the ring and oxygen binding sites for all metals. Tables 5−7 give the calculated vibrational frequencies and radiative intensities for three of these complexes.

Since an important goal of these calculations was to compare the ring and oxygen binding sites, it was important to pay attention to site-dependent differences in zero-point energy (ZPE) and BSSE effects. Vibrational frequencies and ZPE corrections were calculated for a few representative cases, as an indication of their importance. The ZPE corrections act to decrease the binding energies, and are small, amounting to ~1 kcal mol^{-1} for Al^+ and Cr^+ at the ring site, and 0.2 kcal mol^{-1} for Al^+ at the oxygen site. ZPE corrections act to enhance the stability of the oxygen site relative to the ring site by a small amount, on the order of 0.5 kcal mol^{-1}. As an approximate ZPE correction, 1 kcal mol^{-1} was subtracted from all of the ring-site results, and 0.5 kcal mol^{-1} from the oxygen-site results.

The proper way to correct for BSSE and even the appropriateness of doing so are debatable.[65] In a recent assessment of this question, Xantheas[64] emphasized that the conventional "counterpoise" correction[66] should be modified to take geometry relaxation into account, but one can also gather from his work that, for small basis sets, the best approximation to the infinite-basis limit may actually be the binding energy calculated with no BSSE correction. It is generally agreed that counterpoise BSSE corrections indicate the possible extent of this source of systematic error but are not very reliable as actual corrections applied to particular cases. In the present work a number of BSSE correction values were calculated according to the geometry-relaxed prescription of Xantheas.[64] With the basis sets which included diffuse orbitals on the carbons, used in most of these calculations, the BSSE correction was fortunately small, ranging from 0.2 kcal mol^{-1} for Na^+ to 1.2 kcal mol^{-1} for Cr^+. Only for Fe^+, where the smaller basis set was used, were the BSSE corrections large enough to make a significant change in the binding picture. The corrections were either made as calculated or estimated from comparable systems. The values of phenol binding energy corrected for estimated BSSE and ZPE effects are given in parentheses in Table 8.

Results and Discussion

Experimental Observations. Most of the systems studied here showed simple association behavior, with no significant competing reaction processes. Figure 1 shows, for example, the reactions of Cr^+ with indole. For the low-pressure kinetics analysis to be valid, it is necessary to ensure that no significant collisional relaxation of metastable complexes competes with radiative relaxation or else to extrapolate the kinetics to zero pressure. This was checked for all cases by measuring the association rate at several pressures. It was unnecessary to make any extrapolations, since no pressure dependence of the rate constants was found.

Phenol. Reactions of Na^+ and K^+ with phenol were too slow to observe in our experimental regime. Ca^+ did not associate with phenol but underwent fast reactions, forming $CaOH^+$ and $CaOPh^+$. Al^+ formed AlO^+ in amounts comparable with $Al(Phenol)^+$. Association of Fe^+ with phenol proceeded with essentially collisional rate. The metal ions for which the association reaction with phenol was observable yet significantly slower than the collision rate were Cr^+, Mg^+, and Al^+, and experimental results for these ions are given in Table 4. All four systems in Table 4 displayed sequential association ultimately resulting in formation of ML_2^+.

The VTST-based analysis to yield the "experimental" binding energies was straighforward. These are given in Table 4.

The computed results described below probably give the best available comparisons of the ring and oxygen binding sites for the various metal ions. However, some indirect experimental

(65) Stone, A. J. *The Theory of Intermolecular Forces*; Oxford University Press: Oxford, 1995.
(66) Boys, S. F.; Bernardi, F. *Mol. Phys.* **1970**, *19*, 553.

Table 5. Complex-Ion Vibrational Frequencies, Intensities, and Rotational Constants for PhenolAl$^+$, Oxygen Binding Site. B3LYP-DFT Calculations, Augmented 6-31G(d) Basis as Described in the Text

frequency[a] (intensity)		
42(0.5), 66(7.8), 207(121), 217(51), 389(96), 391(1.1), 424(1.2), 491(1.9), 534(24), 624(0.006), 692(18), 765(58), 786(45), 838(0.16), 934(1.6), 984(0.007), 1017(14), 1027(0.05), 1046(4.6), 1108(5.5), 1142(53), 1201(13), 1203(0.02), 1209(21), 1346(0.01), 1364(6.9), 1503(7.4), 1527(32), 1632(0.7), 1656(8.7), 3210(1.1), 3212(0.5), 3219(1.0), 3228(0.2), 3234(0.3), 3721(182)		
rotational constants		
0.14	0.035	0.031

[a] Frequencies and rotational constants in cm^{-1}, intensities in km/mole. Frequencies given here are unscaled, but were scaled downward by 0.99 when used in the kinetics calculations described in the text.

Table 6. Complex-Ion Vibrational Frequencies, Intensities, and Rotational Constants for PhenolAl$^+$, Ring Binding Site. B3LYP-DFT Calculations,[a] Augmented 6-31G(d) Basis

frequency[a] (intensity)		
111(1.5), 136(2.5), 218(60), 237(30), 380(0.5), 415(11), 455(107), 510(17), 536(4.4), 620(0.30), 678(7.2), 814(108), 839(18), 887(1.2), 929(4.3), 1003(0.80), 1007(6.9), 1016(0.90), 1041(1.9), 1095(13.8), 1191(148), 1197(21), 1206(7.8), 1351(83), 1374(3.0), 1381(40), 1501(45), 1544(104), 1609(26), 1640(97), 3201(0.90), 3217(0.34), 3221(1.1), 3230(7.2), 3236(3.3), 3791(145)		
rotational constants		
0.083	0.056	0.052

[a] Frequencies and rotational constants in cm^{-1}, intensities in km/mole. Frequencies given here are unscaled, but were scaled downward by 0.99 when used in the kinetics calculations described in the text.

Table 7. Complex-Ion Vibrational Frequencies, Intensities, and Rotational Constants for PhenolCr$^+$, Ring Binding Site. B3LYP-DFT Calculations, 6-311+G(d) Basis on the Metal

frequency[a](intensity)		
57(1.7), 75(1.5), 201(7), 231(1.4), 409(8.3), 420(3.6), 438(110), 529(12), 531(3.7), 622(0.20), 682(5.2), 807(83), 833(10), 871(1.2), 916(5.0), 986(0.35), 997(4.0), 1008(2.4), 1031(1.4), 1085(13.8), 1187(2.5), 1188(148), 1198(21), 1340(71), 1348(21), 1373(32), 1491(30), 1530(37), 1597(28), 1628(107), 3201(0.90), 3217(0.12), 3223(0.90), 3232(6.1), 3237(2.7), 3801(133)		
rotational constants		
0.080	0.050	0.046

[a] Frequencies and rotational constants in cm^{-1}, intensities in km/mole. Frequencies given here are unscaled, but were scaled downward by 0.99 when used in the kinetics calculations described in the text.

Table 8. Phenol. Calculated Binding Energies and Geometries for M$^+$/Phenol. B3LYP-DFT Calculations. (Values in Parentheses Corrected for BSSE and Vibrational Zero-Point Energy Effects)

	ring		oxygen	
	binding energy (kcal mol^{-1})	M$^+$/ring distance (Å)	binding energy (kcal mol^{-1})	M$^+$/oxygen distance (Å)
Na^+	24.9 (23.7)	2.38	24.9 (24.2)	2.20
Mg^+	32.8 (31.3)	2.30	34.2 (32.9)	2.04
Al^+	32.1 (30.3)	2.37	31.7 (30.8)	2.02
Cr^+	39.2 (37.5)	2.13	37.1 (35.8)	2.04
$Fe^+(d^7)$[a]	66.0[c](62.8[c]), 55.5[d]	1.76	47.9[c](46.1[c]), 37.4[d]	2.01
(d^6s)[b]	46.3[c]		37.7[c]	2.06

[a] Calculated energies of attachment of $Fe^+(^6D)$ to give the d^7 quartet complex. [b] Attachment of $Fe^+(^6D)$ to give the d^6s sextet complex. [c] Direct calculation of sextet Fe^+, attaching to give the designated complex. [d] Indirect calculation, quartet Fe^+ attaching to give the designated complex, corrected by the experimental quartet/sextet energy splitting (5.5 kcal mol^{-1}) of Fe^+.

evidence suggesting that Mg^+ and Al^+ bind at the oxygen site to a significant extent can be found in the data on ML_2^+ formation. Pozniak and Dunbar[39] found that these two metals do not form sandwiches ML_2^+ when binding at the coronene π-face. Similarly, no sandwich was found for[67] Al^+ or[41b] Mg^+ reacting with benzene. This pattern is also clear for indole, where the binding is certainly on the π-site, and where Mg^+ and Al^+

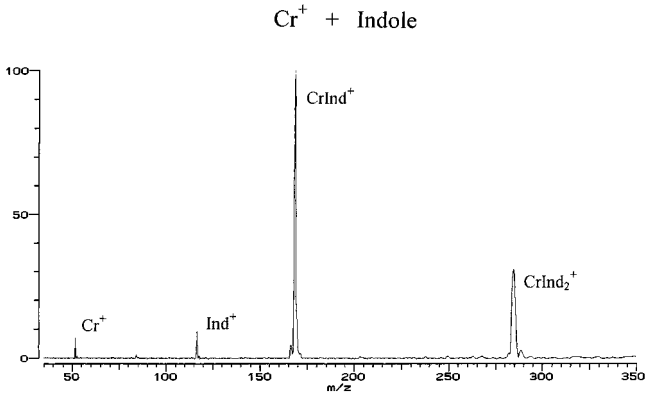

Figure 1. Association of Cr^+ with indole at an indole pressure of 2×10^{-7} Torr. Reaction time 20 s.

form no observable ML_2^+ dimer complexes. In contrast, phenol and *p*-cresol form ML_2^+ species with Mg^+ and Al^+ at substantial rates (see Table 4). This strongly contrasting behavior suggests the possibility that these two metal ions sit on the oxygen sites of these two molecules, although it is certainly not necessary to postulate an oxygen-bound structure for ML^+ in order to

(67) Stöckigt, D.; Hrušák, J.; Schwarz, H. *Int. J. Mass Spectrom. Ion Processes* **1994**, *149/150*, 1.

rationalize formation of an ML_2^+ structure with one or both ligands oxygen-bound to the metal ion.

Other evidence, also indirect, suggesting involvement of the oxygen binding site in phenol is the observation that Ca^+ reacts with with phenol to give $CaOH^+$ and $CaOPh^+$. This set of products is most easily rationalized by initial attack of calcium ions at the oxygen site, which in this case leads to exothermic reaction rather than stable complex formation. Similarly the substantial formation of AlO^+ suggests at least some extent of attack at the oxygen.

Indole. Reactions of Na^+ and K^+ with indole were slow but observable. The association adducts with these two ions once formed did not react any further. Ca^+ reacted with indole with 10% efficiency and slowly formed an ML_2^+ species. Mo^+ reacted three times faster than Ca^+ and formed ML_2^+ very fast. Reactions of Mg^+, Al^+, Cr^+, and Fe^+ with indole were very fast (near the collision rate). ML^+ species of Cr^+ and Fe^+ quickly formed ML_2^+ complexes, while ML^+ species of Mg^+ and Al^+ reacted further with indole by hydrogen abstraction, forming MLH^+. Association results for these systems are summarized in Table 4.

For Na^+/indole (Table 3), K^+/indole, and Ca^+ the vibrational properties were available to permit a VTST-based determination of the binding energy. For the other metal ions, the analysis was done using the approximate standard hydrocarbon approach,[45] which has been found to be quite successful for atomic ion/aromatic neutral associations[34,36] (see Table 1). The binding energies assigned to these systems are given in Table 4.

Experimental Comparison of Indole with Naphthalene. Naphthalene is a 10 π-electron homocyclic analogue of indole, and it is interesting to compare the relative binding to metal ions. The main difference between them is the dipole moment of indole directed from the nitrogen across the center of the molecule to the opposite end of the benzene ring, corresponding to the flow of π-electrons away from the nitrogen lone pair. The ab initio calculations of Mecozzi et al.[13] for Na^+, and those of our group for other metal ions,[21] indicate that the best binding site of indole is over the phenyl ring, toward the negative end of the dipole. Our calculations indicated the indole binding energy for Na^+ to be 5 kcal mol^{-1} higher than that of naphthalene, while ref 13 indicated an enhancement of 3.9 kcal mol^{-1}. An experimental comparison was made here between the Na^+/indole and Na^+/naphthalene systems. The association rate with indole corresponds to a binding energy of 34 kcal mol^{-1} (either StH or VTST analysis). Association with naphthalene was measured to be 0.7% efficient, corresponding to a binding energy of 30 kcal/mol (StH). This experimental 4 kcal mol^{-1} binding energy enhancement for indole is in good agreement with the calculated enhancement.

Binding of Cr^+ to these two π-faces was also compared. Unfortunately the association reactions were both too fast to derive useful values of binding energy from the RA kinetics. To make at least a qualitative comparison, CID was performed on the mixed indole−naphthalene complex with Cr^+. The CID spectra at different rf excitation amplitudes are shown in Figure 2. The dissociation leads predominantly to formation of $CrInd^+$ ions. Although no $CrNaph^+$ complex was observed, a small Ind^+ peak is present which could represent breakage of the Cr−Ind bond with the charge staying on Ind^+ instead of $CrNaph^+$. This sets as a lower limit that 75% or more of CID cleavages break the Cr^+−naphthalene bond. Although we are not able to obtain quantitative information on binding energies through this technique, the indicated higher binding energy of indole relative to naphthalene confirms our qualitative expectation.

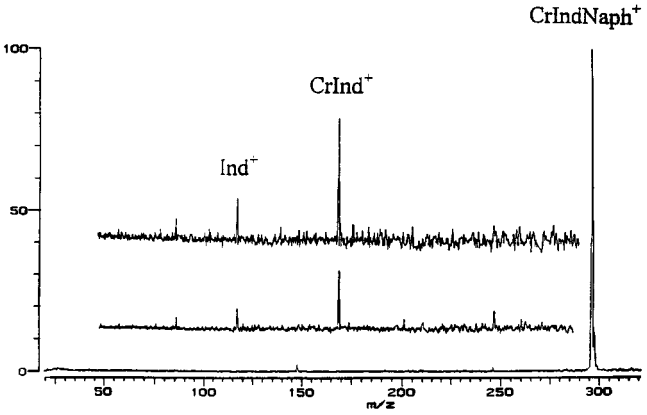

Figure 2. Competitive CID of Cr(Indole)(Naphthalene)$^+$ complex at different rf amplitudes. The lowest trace is the spectrum without rf excitation, and the middle and upper traces are CID spectra at progressively higher rf amplitudes, corresponding to progressively higher parent ion velocities. (The small peak at *m*/*z* 148 is a detection artifact, specifically a harmonic peak.) The preferential loss of naphthalene indicates a higher binding energy to indole.

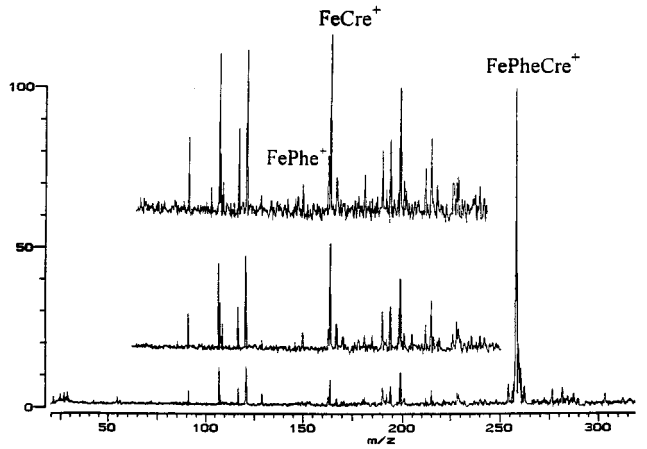

Figure 3. Competitive CID of Fe(Phenol)(*p*-Cresol)$^+$ complex at different amplitudes. The three traces have the same significance as described for Figure 2. Illustrates higher binding energy of *p*-cresol relative to phenol.

Cresol. In Tyr and Trp, the respective phenol and indole fragments are attached to the α-carbon through a $-CH_2$ group; compared to phenol and indole as models, this causes some perturbations to the dipole moment and π-electron distribution in the aromatic fragment. These changes should be taken into account if one wants to compare metal ion binding in peptides with binding in fragment models. An obvious first step is the comparison of phenol with *p*-methylphenol (*p*-cresol). Association of Mg^+, Cr^+, and Fe^+ with *p*-cresol proceeded at near collisional rate, telling us at least for Mg^+ and Cr^+ that the binding is substantially stronger than for phenol. In the cases of Fe^+ and Cr^+, the stronger binding of *p*-cresol relative to phenol was confirmed by the competitive CID method. Figure 3 presents a CID spectrum of a mixed complex of Fe^+ with phenol and *p*-cresol, showing a production of Fe(*p*-cresol)$^+$ fragments clearly larger than Fe(phenol)$^+$ fragments. A similar CID of the Cr(*p*-cresol)(phenol)$^+$ complex also indicated a higher binding energy of *p*-cresol than phenol. For Cr^+ at least, the enhancement of binding by methyl substitution has some precedent: Measurements of the Cr^+ binding energies to benzene and methyl-substituted benzenes[32] suggested that the

addition of a new methyl group increases the binding energy by 2−3 kcal mol^{-1}, although the uncertainties of these measurements were rather large.

Quantum-Chemical Results. Recent calculations of binding of several cations to phenol and indole have been reported, including alkali ions and ammonium ions.[3,12,13,15,20] The present calculations may be of interest for several reasons: first, comparable results are reported for a wider variety of cations, including open shell and transition-metal ions; second, the present B3LYP-DFT approach with a more flexible basis gives an interesting comparison with previously published results using Hartree−Fock or MP2 methods without diffuse functions in the basis; and third, the possibilities of alternative heteroatom binding sites are more fully explored here.

Phenol. The phenol calculations showed two well-defined metal ion binding sites for all of the metals studied. Table 8 shows the binding energies and metal/ligand distances for these two sites. The π-face site over the ring is similar to that well-known for benzene and other aromatics, with the metal ion nearly over the center of the benzene ring. The oxygen site was always found to be a stable minimum on the potential surface, although the barrier to interconversion to π-site binding was not explored. The oxygen site might have been expected to be nearly "tetrahedral" (with the oxygen lone pair occupying the fourth vertex), but the calculated geometry actually corresponded poorly to such an idea, except for Fe^+, which had reasonably good tetrahedral geometry around the oxygen. For all of the other cases, the metal ion lies almost directly over the oxygen, with a C−O−M$^+$ angle of roughly 90°, and the O−M$^+$ direction virtually perpendicular to the plane of the ring. This geometry corresponds more closely to the idea of the metal ion coordinating to a pure p_z orbital on oxygen.

Fe^+, with its partly filled d orbitals and low-lying excited state, poses particular problems for the calculations and the interpretation. The high-spin ^6D ($3d^64s^1$) state is known to be the ground state of the isolated ion, and experimentally this state is 5 kcal/mol *more stable* than the low-spin ^4F ($3d^7$) excited state.[68] However, the B3LYP-DFT calculation with the 6-311+G(d) basis gives the ^6D state as *less stable* than the ^4F state by 5 kcal/mol. Thus this method clearly has difficulty with the relative positioning of the quartet and sextet manifolds.

This is particularly troublesome for the present system, because binding of Fe^+ to π-sites almost certainly involves a spin change to give a quartet spin state of the complex based on the following considerations: For benzene, Bauschlicher[69] found the quartet complex to be more stable than the sextet complex by about 6 kcal/mol. For phenol, the energetic advantage of the quartet complex seems to be larger than that for benzene, so that the present calculations gave the quartet complex with phenol as somewhere between 8 and 19 kcal/mol more stable than the sextet complex (depending on the assumptions made, see the next paragraph). These differences in favor of the quartet complex are large enough that there is little doubt about the spin change upon π-face complexation of Fe^+ to phenol. Thus, the calculation of the binding energy of Fe^+ to give the ground-state complex must take into account the rather unsatisfactory confidence of the B3LYP-DFT comparison of the quartet and sextet manifolds.

Two procedures seem defensible. One is to take the B3LYP-DFT binding energy (66 kcal mol^{-1}, not including BSSE corrections) at face value, on the presumption that the B3LYP-DFT calculation will be accurate for the *ground states* of both bare ion and complex. The other procedure is to take the calculated value for the attachment of quartet Fe^+ to phenol (61 kcal mol^{-1}) and to correct this by subtracting the experimental energy of the spin flip from sextet to quartet Fe^+, yielding a net binding energy estimate of 55.5 kcal/mol. The latter procedure assumes that the B3LYP-DFT calculations are accurate within the quartet manifold for comparison of (excited state) quartet Fe^+ with (ground-state) quartet phenol complex. We are unable to judge which of these procedures is more likely to be correct, and we give both sets of values below. We can note that the experiment indicates the binding energy to be high, >57 kcal mol^{-1}. This is consistent (within the uncertainties) with the calculated ring-site binding energy assigned by either procedure. For comparison of the two binding sites, we can more confidently compare the B3LYP-DFT values for the quartet complexes, on the assumption that any absolute error deriving from the B3LYP-DFT computation will be similar for the two structures. The ring site is calculated to be so much more stable than the oxygen site for Fe^+ that this ordering holds true regardless of the method chosen to assign the B3LYP-DFT binding energies.

The calculated binding energies for the two sites are given in Table 4. The absolute binding energies derived at this level of calculation are rather uncertain and should probably not be considered better than an uncertainty of ±5 kcal mol^{-1}. Moreover, as discussed below, the B3LYP-DFT method probably underestimates the binding energies by ~5 kcal mol^{-1}. Comparison between different metals with the same level of calculation should be more accurate, as should comparisons of a given metal ion with different neutral ligands. Comparing the two binding sites for the same metal ion should be even more meaningful, and we might hope for an accuracy of 1−3 kcal mol^{-1} for such comparisons.

The calculations indicate that the ring and oxygen sites are similar in energy for the nontransition metal-ions. Which site is actually more stable is generally undecided within the uncertainties of the calculations. The presence of active d orbitals enhances binding to the ring π-site, slightly for Cr^+ and dramatically for Fe^+, in comparison with the main group metal ions. The enhanced π-site binding for the transition-metal ions is also clearly evident in the bond distances: although Mg^+, Al^+, Cr^+, and Fe^+ all have similar metal-to-oxygen distances (oxygen binding site), the two π-bound transition-metal ions have much shorter metal-to-ring distances than the two nontransition-metal ions (ring-binding site).

Indole. The newly calculated B3LYP-DFT binding energies and the MP2 values from ref 21 are both given in Table 9 for the three nontransition-metal ions. The B3LYP-DFT values are noticeably below the MP2 results. This is not surprising. As discussed below, the B3LYP-DFT values are probably systematically low by 5 kcal mol^{-1}. Moreover, the absolute MP2 binding energies from ref 21 are very likely too high, since

Table 9. Indole. Calculated Binding Energies of Metal Ions to Indole (kcal mol^{-1}) (Density Functional and ab Initio Methods). Values in Parentheses Are Corrected for BSSE

	B3LYP-DFT	MP2[a]
Na^+	30.4 (30.2)	36
K^+	20.9 (20.7)	
Mg^+	40.9 (40.5)	51
Al^+	40.2 (39.8)	50
Cr^+	45.1 (44.5)	

[a] From ref 21.

(68) Moore, C. E. *Atomic Energy Levels as Derived from the Analyses of Optical Spectra*; National Bureau of Standards: Washington, D. C., 1971; Vol. NSRDS-NBS 35.

(69) Bauschlicher, C. W., Jr.; Partridge, H.; Langhoff, S. R. *J. Phys. Chem.* **1992**, *96*, 3273.

BSSE errors were not corrected, and are expected to be substantial for these MP2 calculations.

For Mg^+, the MP2 results of ref 21 suggested (in contrast to the other metal ions) that there might be a shallow local energy minimum for Mg^+ located approximately over the nitrogen atom. This possibility was reinvestigated by B3LYP-DFT calculations, and no energy minimum was found. Moving from the pyrrole binding site toward the nitrogen atom, the energy is seen to increase slowly but monotonically such that, when the Mg^+ is directly over the nitrogen, the energy is higher by 3.3 kcal mol^{-1} than at the pyrrole binding site. There is thus no good indication of a stable lone-pair binding site at the nitrogen for any metal ion that has been studied.

General Discussion. The new experimental results reported here add to the small body of information about metal ion binding energies to these two molecules. Values using the full VTST calculation are reported for Al^+, Mg^+, Cr^+, and Fe^+ (lower limit) with phenol, and for Na^+, K^+, and Ca^+ with indole. Binding energies (Mg^+, Al^+) and lower limits (Cr^+, Fe^+, Mo^+) are also estimated for indole by StH modeling.

Addition of a second ligand to both phenol and indole to form ML_2^+ (Table 4) is rapid for the transition metals, in accord with the expectation based on previous work with benzene and naphthalene. Looking at the nontransition metals, a notable contrast with benzene chemistry is the fact that Mg^+ ($3s^1$) and Al^+ ($3s^2$) form dimer complexes with phenol at a substantial rate. The failure of benzene to form dimer complexes with these two metal ions has been attributed to the polarization of the valence electron(s) of the metal away from the π-bound first benzene ligand, leading to unfavorable π interaction with a second incoming ligand.[70] The formation of dimer complexes of these ions with phenol very likely reflects the availability of the oxygen binding site on one or both of the phenol ligands, so that dimer complexes which do not have the unfavorable structure of two π-ligands in sandwich configuration around the metal are possible.

Indole follows the expectation from the benzene analogy in that no dimer complexes are observed with the nontransition metals Na^+, K^+, Mg^+, or Al^+. The surprise in this case is the rapid formation of dimer complexes with Ca^+ ($4s^1$), which is a striking contrast with Mg^+. Evidently the larger size of Ca^+ accommodates binding of the second π-ligand in a way that Mg^+ cannot.

The combination of experimental and quantum-chemical information from this work along with literature values for benzene allows quite solid conclusions about binding energies of a variety of metal ions binding to phenol and indole. Table 10 represents the thermochemical conclusions we can reach for several metal ions. While the ab initio and B3LYP-DFT values of absolute binding energies are rather uncertain, they are more useful when taken relative to the corresponding calculated binding energies to benzene, which are known with reasonable confidence. This is particularly true for Fe^+, where the presence of a low-lying excited state of different multiplicity makes the calculation of absolute binding energies very uncertain but where it is still possible to make a useful comparison between similar benzene and phenol calculations. The experimental radiative association kinetics-derived values are expected to be valid as absolute measurements and hence provide a useful anchor for the quantum-chemical calculated values. The best estimates given in Table 10 for phenol and indole accordingly rely on experimental values and on direct quantum-chemical comparisons with benzene.

Table 10. Best-Estimate Binding Energies for Representative Metal Ions with Benzene, Phenol, and Indole (kcal mol^{-1}) Based on Available Experimental Evidence, Supplemented by Quantum Chemistry Comparative Estimates

	benzene	phenol	indole
Na^+	28 ± 1^a	28 ± 3^f	34 ± 3^l
K^+	19 ± 1^b	20 ± 3^f	25 ± 3^m
Al^+	35 ± 2^d	37 ± 4^g	45 ± 4^n
Mg^+	35 ± 3^c	38 ± 4^h	46 ± 4^p
Cr^+	40 ± 3^e	43 ± 4^i	47 ± 4^f
Fe^+	49 ± 3^e	60 ± 6^k	$(>48)^q$

[a] Experimental (ref 72). [b] Experimental (ref 73). [c] Calculated with estimated corrections, ref 74. (Our uncertainty estimate.) [d] Experimental/theoretical (refs 22,36). [e] Experimental (ref 56). [f] B3LYP-DFT calculation, present work, relative to benzene. [g] B3LYP-DFT calculation, present work, relative to benzene (1.4 kcal mol^{-1} larger than benzene), combined with with the present experimental value. [h] Present experimental value relative to Al^+. Oxygen site assumed. [i] Compared with Cr^+ binding to benzene, B3LYP-DFT results indicate 1.5 kcal mol^{-1} stronger binding to phenol, while radiative association kinetics indicate 5 kcal mol^{-1} stronger binding to phenol. These results are averaged here. [k] B3LYP-DFT calculation relative to benzene (10.5 kcal mol^{-1} higher than benzene), supported by the experimental lower limit in Table 4. [l] Present experimental results supported by quantum-chemical results relative to benzene (MP2 calculation 6.5 kcal mol^{-1} higher than benzene, ref 21) present B3LYP-DFT calculation 6 kcal mol^{-1} higher than benzene). [m] B3LYP-DFT calculation relative to benzene (6 kcal mol^{-1} higher than benzene), in agreement with the present experimental results. [n] MP2 (ref 21) and B3LYP-DFT calculations relative to benzene. [p] Calculations (present and ref 21) relative to Al^+. [q] Lower limit from present experiment.

For the nontransition-metal ions, phenol appears to be comparable to or slightly higher than benzene in binding strength (as was previously calculated and discussed for the Na^+ case [13]). The transition metals may be different in this respect: Cr^+/phenol binding may be somewhat enhanced, whereas for Fe^+ the calculations suggest substantially enhanced binding to phenol relative to benzene. The present experiments strongly indicate that phenol is a much better ligand than benzene for Cr^+, since the radiative association in the former case is 14 times as efficient as in the latter case. This leads to the assignment of the experimental Cr^+/phenol binding energy as 5 kcal mol^{-1} higher than the benzene binding energy. It will be interesting in future work to see whether enhanced phenol binding compared with benzene holds true for other strongly interacting transition-metal ions.

Indole is bound to all of the metal ions more strongly than benzene, with an enhancement of 5−10 kcal mol^{-1}. The analysis in ref 21 suggests that this enhancement is attributable to comparably sized contributions of two effects, namely, the larger size of the π-system and the favorable interaction of the cation with the indole dipole.

The electrostatic point of view advanced by the Dougherty group[3,4,12,13] for understanding binding energy differences in sodium ion systems is equally valid for the other nontransition-metal ions considered here, and we can briefly recapitulate a few points. The similarity of phenol and benzene reflects the fact that the local dipolar charge distribution in phenol is oriented such that it gives little electrostatic help to a cation sitting at the ring π-binding site (this is essentially the OH dipole, which is nearly perpendicular to the C−O bond[71]). By contrast, the

(70) Bauschlicher, C. W., Jr.; Partridge, H. *J. Phys. Chem.* **1991**, *95*, 9694.

(71) Minkin, V. I.; Osipov, O. A.; Zhdanov, Y. A. *Dipole Moments in Organic Chemistry*; Plenum Press: New York, 1970.

(72) Guo, B. C.; Purnell, J. W.; Castleman, A. W., Jr. *Chem. Phys. Lett.* **1990**, *168*, 155.

(73) Keesee, R. G.; Castleman, A. W., Jr. *J. Phys. Chem. Ref. Data* **1986**, *15*, 1010.

(74) Bauschlicher, C. W., Jr.; Partridge, H. *Chem. Phys. Lett.* **1991**, *181*, 129.

dipole in indole is well oriented such that a cation at the phenyl π-site sees substantial electrostatic stabilization, resulting in markedly enhanced cation binding relative to benzene or naphthalene. Similarly, the contrasting situation regarding existence of a binding site on the heteroatom of these two molecules can be understood in terms of their different charge distributions. The local buildup of negative charge near the oxygen of phenol leads to a lone-pair binding site above the oxygen whose stability is similar to the π-site for nontransition-metal ions. In contrast, the positive charge accumulation in the nitrogen region of indole makes cation binding there unfavorable, and no reasonable lone-pair nitrogen binding site on indole has been identified for any of the metal ions studied. However, these purely electrostatic ideas apparently must be supplemented for transition-metal ions with active d orbitals and electons. As seen above, the Cr^+ and particularly the Fe^+ systems show evidence for specific interactions and enhanced binding with the π-sites not fully accounted for by electrostatic arguments.

These data give an opportunity to evaluate the accuracy of the quantum-chemical calculations for several cases. Comparison between Tables 4 and 8 gives corresponding experimental and quantum chemical values for phenol bound to Mg^+, Al^+, and Cr^+. In addition, the B3LYP-DFT computed values for binding Na^+, K^+, Al^+, and Cr^+ to benzene, which are 24, 15, 30, and 37 kcal mol^{-1}, respectively, can be compared with previously known experimental values (given in Table 10). It can be seen that the B3LYP-DFT results consistently give smaller binding energies to phenol and benzene than experiment, by amounts ranging from 3 to 10 kcal mol^{-1}. Similarly, comparison of Tables 4 and 9 for Na^+, Mg^+, Al^+, and Cr^+ binding to indole indicates that B3LYP-DFT underestimates the experimental binding energies by 3−8 kcal mol^{-1}. Although the experimental values should be considered as uncertain within several kcal mol^{-1}, nevertheless this trend is so consistent that it seems quite likely that this DFT quantum-chemical approach gives systematically low absolute binding energies for these π-complexes. Strongly supporting this are the calculations of Stöckigt[22] for aluminum ion binding to several monocyclic π molecules, which suggested that B3LYP-DFT results using an adequate basis were systematically ~5 kcal mol^{-1} too low for this metal ion.

On the other hand, the MP2 calculated values for Na^+, Mg^+, and Al^+ binding to indole (Table 9) are several kcal mol^{-1} higher than the experimental values. Those values were not corrected for BSSE, which is certainly substantial for MP2-level calculations with the modest basis set used, and it is likely that these values corrected for BSSE would be reasonably close to the experimental values.

Overall, it is not reasonable to expect good absolute binding energies from calculations at this level of computation. Cubero et al.[15] remark that the good values of Na^+ binding obtained with HF/6-31G** calculations "probably result from fortuitous error cancellation." MP2 calculations might be somewhat better than this, and B3LYP-DFT calculations might also be better if an empirical correction of 5 kcal mol^{-1} is added to the values, but the expectation, confirmed by the present poor absolute values from the DFT calculations, is that absolute binding energies calculated with these levels of theory are not reliable to better than several kcal mol^{-1}. The point of view we have taken to justify the interpretations in the present study is that *relative* calculations for the same metal ion can be compared with considerably greater confidence.

Conclusions

The radiative association kinetics approach was applied successfully to measure and compare metal ion binding energies of a variety of gas-phase cations to phenol and indole. It was possible to carry out detailed VTST-based modeling in deriving binding energies from kinetics data for many of the systems, and the standard hydrocarbon modeling approach was applied to estimate binding energies for several additional systems.

Combining our experimental and quantum-chemical approaches with literature information leads to binding energy assignments for a variety of metal cations binding to phenol and indole. Where there is overlap, relative binding energies from experiment and from theory are generally concordant, although the absolute binding energies from the B3LYP-DFT calculations are consistently lower than the experimental values. For indole, binding to the π-face at the phenyl end of the molecule is always substantially more favorable than alternative possibilities. For phenol, binding to the π-face is never much weaker than the oxygen site, but for nontransition metals, and nearly so for Cr^+, binding to the lone pair on the oxygen is competitive with the π-site within the uncertainty of the calculations. Binding to phenol is generally just slightly stronger than binding of the same metal ion to benzene for the nontransition metals, but the Cr^+ and Fe^+ results suggest that transition-metal ions have enhanced π-binding to phenol. Indole is a better ligand than phenol by 4−10 kcal mol^{-1}, reflecting both the better π-binding ability of the expanded naphthalene-like π-system and the electrostatic stabilization provided by the favorably oriented dipole moment.

Addition of a second ligand to form ML_2^+ generally follows the precedent of benzene, with ready dimer ion formation for transition metals, but not for nontransition metals (Ca^+ being exceptional). However, $Al^+$and Mg^+ with phenol break this pattern, suggesting the possibility of oxygen-site binding being involved in these two dimer complexes.

B3LYP-DFT calculations using a basis including diffuse functions appear to perform well in mirroring the experimental binding energy patterns, but the absolute binding energies from this method appear to be systematically lower than experiment.

Acknowledgment. The advice and help of Professor Stephen Klippenstein was invaluable in carrying out this project. Support is acknowledged from the National Science Foundation and from the donors of the Petroleum Research Fund, administered by the American Chemical Society.

JA983272Z